

Objective Evaluation of Functionality of Filtering Bleb Based on Polarization-Sensitive Optical Coherence Tomography

Deepa Kasaragod,¹ Shinichi Fukuda,² Yuta Ueno,² Sujin Hoshi,² Tetsuro Oshika,² and Yoshiaki Yasuno¹

¹Computational Optics Group, University of Tsukuba, Tsukuba, Japan

²Department of Ophthalmology, Faculty of Medicine, University of Tsukuba, Tsukuba, Japan

Correspondence: Yoshiaki Yasuno, Computational Optics Group, University of Tsukuba, Tsukuba 305-0821, Japan; yasuno@optlab2.bk.tsukuba.ac.jp.

Submitted: September 12, 2015

Accepted: February 5, 2016

Citation: Kasaragod D, Fukuda S, Ueno Y, Hoshi S, Oshika T, Yasuno Y. Objective evaluation of functionality of filtering bleb based on polarization-sensitive optical coherence tomography. *Invest Ophthalmol Vis Sci*. 2016;57:2305-2310. DOI:10.1167/iops.15-18178

PURPOSE. The fibrosis score is a new diagnostic score that we have developed to evaluate the function of bleb structures after glaucoma filtration surgery using polarization-sensitive optical coherence tomography (PS-OCT). This study aims to assess the efficacy of the fibrosis score in discriminating nonfunctional from the functional blebs.

METHODS. A total of 20 patients who had undergone glaucoma filtration surgery were imaged at different time periods after surgery using PS-OCT. Birefringence tomography of blebs was obtained from PS-OCT, and the fibrosis score was computed for each patient. The fibrosis score is defined as the area of occupation of high birefringence area in the conjunctiva. The blebs were classified as functional or nonfunctional according to the IOP and the application of medication. The power of the fibrosis score to discriminate nonfunctional blebs from functional blebs was evaluated.

RESULTS. The difference in the mean fibrosis score between the functional and nonfunctional bleb group was statistically significant. The fibrosis score showed good ability to discriminate nonfunctional from functional blebs. The area under the receiver operating characteristic curve was 0.82. The best combination of the sensitivity and specificity was 67% and 100%, respectively, for classifying nonfunctional cases.

CONCLUSIONS. The fibrosis score showed a high ability to discriminate nonfunctional from functional blebs. Polarization-sensitive OCT is a noninvasive technique that provides not only the fibrosis score but also standard structural tomography. It can be a comprehensive tool for longitudinal evaluation after filtration surgery for glaucoma.

Keywords: polarization-sensitive optical coherence tomography, birefringence, fibrosis, trabeculectomy, bleb, anterior segment, glaucoma filtration surgery

Filtration surgeries, including trabeculectomy and Ex-PRESS shunt surgery, are a common choice for IOP control of glaucoma.¹ The favorable outcome of filtration surgery is determined by the proper functioning of the filtration structure called the bleb, and it is highly dependent on postoperative tissue alterations, including fibrosis and scarring. These fibrosis and scarring processes, sometimes along with dome-shaped encapsulation of the bleb, can result in the blockage of aqueous flow and poor maintenance of IOP. Hence, the inhibition of wound healing is an indication of successful filtration surgery.^{2,3}

Despite recent improvements in surgical techniques,⁴⁻⁶ fibrosis is inevitable in the long-term, and a good monitoring scheme is required to optimize the reintervention and follow-up medication. The current follow-up modalities include color photography,⁷ slit-lamp examination,⁷ ultrasound biomicroscopy (UBM),⁸ in vivo confocal microscopy,⁸ and anterior segment optical coherence tomography (AS-OCT).^{9,10} Color photography and slit-lamp examination are easy and widely available, but do not provide depth-resolved information. Although UBM provides depth-resolved information, it is a contact measurement modality. Laser scanning in vivo confocal microscopy

provides high resolution, but with only limited depth penetration. Bleb features detected by AS-OCT were shown to be correlated with its functionality.^{9,10} However, it cannot directly contrast and quantify the fibrosis and scarring.

Understanding the morphologic evolution of blebs would improve the success rate of the filtration surgery. Several bleb evaluation and classification schemes have been used. Wells et al.¹¹ used color photographs and clinical examination to evaluate the various bleb morphologic parameters. The Indiana Bleb Grading Appearance Scale (IBAGS)¹² and Moorfields Bleb Grading System (MBGS)^{7,11} are two examples of recent bleb classification systems. Although clinical relevance has been established with these schemes, the assessment mainly follows morphologic investigation.

An evaluation method accounting for the tissue property would improve the long-term monitoring and classification of the bleb. Polarization-sensitive OCT (PS-OCT) is an extension of OCT that is capable of noninvasively measuring the polarization property of the bleb. Since the fibrosis and scarring are associated with abnormal growth of collagen, and collagen is known to have strong birefringence, PS-OCT can reveal the fibrosis and scarring of the bleb. Previous studies have shown



that phase retardation tomography of the bleb obtained by PS-OCT provide information associated with fibrosis and scarring of the bleb.^{13,14} Recently, Fukuda et al.¹⁵ reported a high correlation of phase retardation alteration with bleb function. They also have performed a small cohort size follow-up study and found that the increase in IOP was preceded by the alteration of phase retardation.¹⁵

Despite this strong relationship between the phase retardation and functionality of the bleb, the phase retardation does not accurately provide the depth-localized polarization property of the bleb. This has restricted further development of PS-OCT applications for bleb analysis. This limitation has been highlighted by our theoretical study, and a new localized analysis method recently was devised to overcome it.^{16,17}

We applied this birefringence imaging to evaluate blebs. We define a new metric called the fibrosis score (FS) to quantify the progression of fibrosis and scarring based on the birefringence values of the bleb. We examined the capability of the FS to classify blebs as functional or nonfunctional by investigating 20 bleb cases.

PATIENTS AND METHODS

Polarization Sensitive OCT

The PS-OCT used in this study is based on Jones-matrix OCT (JM-OCT) technology, which uses two input polarization states of a probe beam and measures the full information of the polarization property of a tissue.^{14,18,19} The polarization property is represented as a tomography of Jones matrices. Our PS-OCT is a swept source-based system with an operating wavelength of 1.3 μm , a measurement speed of 30,000 A-lines/s, and axial and lateral resolutions in air of 12.7 and 20.5 μm , respectively. The system was specifically designed for imaging of the anterior eye segment. Details of this PS-OCT system have been described previously.¹⁴

The conventional output obtained from JM-OCT is a quantity called cumulative phase retardation. It provides the depth-cumulative polarization property of the tissue. The polarization property measured at a certain depth in the tissue is affected by the all superior tissues above the measured point. In contrast, a truly depth-resolved polarization quantity called birefringence is derived via local Jones matrix approach in this study.¹⁶ This algorithm provides a quantity called birefringence. It is defined as the difference of refractive indices of the orthogonally polarized ordinary and extraordinary light beams in optically anisotropic materials. The birefringence is a depth-localized polarization property of the tissue that is not affected by superior tissue. In practical implementation of local Jones matrix algorithm, a thin but nonzero depth-extent of tissue region is used to compute a birefringence of a single point. In our particular implementation, it is 36 μm (6-pixel depth).

The raw birefringence value obtained from JM-OCT suffers from SNR-dependent systemic bias. This bias is removed using a mathematical method called the maximum a-posteriori (MAP) birefringence estimator.¹⁷ This estimator provides not only an estimated birefringence value, but also its reliability (likelihood). The birefringence and reliability were used in our study. This estimator uses a set of pixels to compute the birefringence and estimation. In our particular implementation, neighboring 3×3 pixels (18 μm [depth] \times 70 μm [lateral]) are used to estimate the birefringence and reliability of the center pixel of the 3×3 pixel region.

Finally, the lateral resolution of the birefringence measurement is defined by the MAP birefringence estimator as 70 μm . On the other hand, the depth resolution is dominated primarily

by the local Jones matrix algorithm, 36 μm , but it would be slightly worsened by MAP birefringence estimator.

Fibrosis Score

We introduce a new objective diagnostic metric, called the FS, which reflects the progression of fibrosis and scarring of blebs. Fibrosis score is computed from the birefringence tomography, and represents the occupancy of the highly birefringent area in the conjunctiva of a bleb. The main rationale behind the FS is that the sclera is composed mainly of collagen fibers and, thus, shows high birefringence, while the conjunctiva contains less collagen and shows low birefringence.^{20,21} Hence, any abnormally high birefringence in the conjunctiva could be attributed to fibrosis or scarring.^{22,23}

To define abnormally high birefringence, we have to first obtain the reference distribution of normal birefringence in the conjunctiva and sclera. From this, we can define a birefringence threshold to divide the normal scleral and conjunctival regions. Any birefringence in the conjunctiva exceeding the birefringence threshold then can be regarded as abnormally high.

To establish the reference birefringence distribution, the superior-anterior segments of 10 subjects without any marked ocular disorders (10 fellow eyes of 10 cataract surgery patients, five males and five females) were measured by PS-OCT. The mean age was 69.2 ± 9.5 years and the mean IOP was 12.8 ± 2.3 mm Hg. The measurement was performed with a horizontal fast raster scanning protocol consisting of 512 (horizontal) \times 128 (vertical) A-lines in a transversal region of 12 \times 12 mm. A region-of-interest (ROI) was selected in each horizontal cross-sectional image (B-scan). The ROI covered the full horizontal extent from the air-tissue interface to the 100-pixel depth (613 μm in tissue), it comprised conjunctiva as well as sclera.

The method of Otsu²⁴ was applied to the birefringence distribution of the ROI, and it provided the optimal birefringence threshold value that separates the two birefringence classes of the conjunctiva and sclera. This method defines the threshold to minimize the intraclass variance between the two birefringence classes. Average birefringence threshold values obtained from 10 subjects then were used to compute the FS. In this particular study, the birefringence threshold was 0.00109.

The first step in computing the FS of individual bleb cases was to delineate the boundary between the conjunctiva and sclera. This was performed manually using the scattering OCT B-scans. If the boundary was not clearly seen in the B-scan, the neighboring B-scans also were observed to delineate the boundary. For some cases, a volumetric OCT obtained by a commercially available anterior OCT (CASIA; Tomey Corp., Aichi, Japan) also is observed as a reference. For these cases with unclear boundary, the delineated boundary is verified by three ophthalmologists (FS, YU, and SH). The OCT B-scans were obtained simultaneously with the birefringence tomography and, therefore, were perfectly coregistered with it. The conjunctival pixels with higher birefringence-estimation-reliability¹⁷ than the predefined threshold were classified as valid pixels. The conjunctival pixels that possessed higher birefringence than the previously-computed birefringence threshold, and higher reliability than the reliability threshold then were classified as fibrotic pixels. The FS finally was defined as $\text{FS} = (\text{number of fibrotic pixels})/(\text{number of valid pixels}) \times 100$ (%). Thus, FS is an occupancy of fibrotic region in the conjunctiva. In this study, the reliability threshold was empirically defined as 0.005. This threshold was defined to include only the tissue pixels and not to include noisy pixels and fluid regions. The reliability threshold also allows us not to include the internal

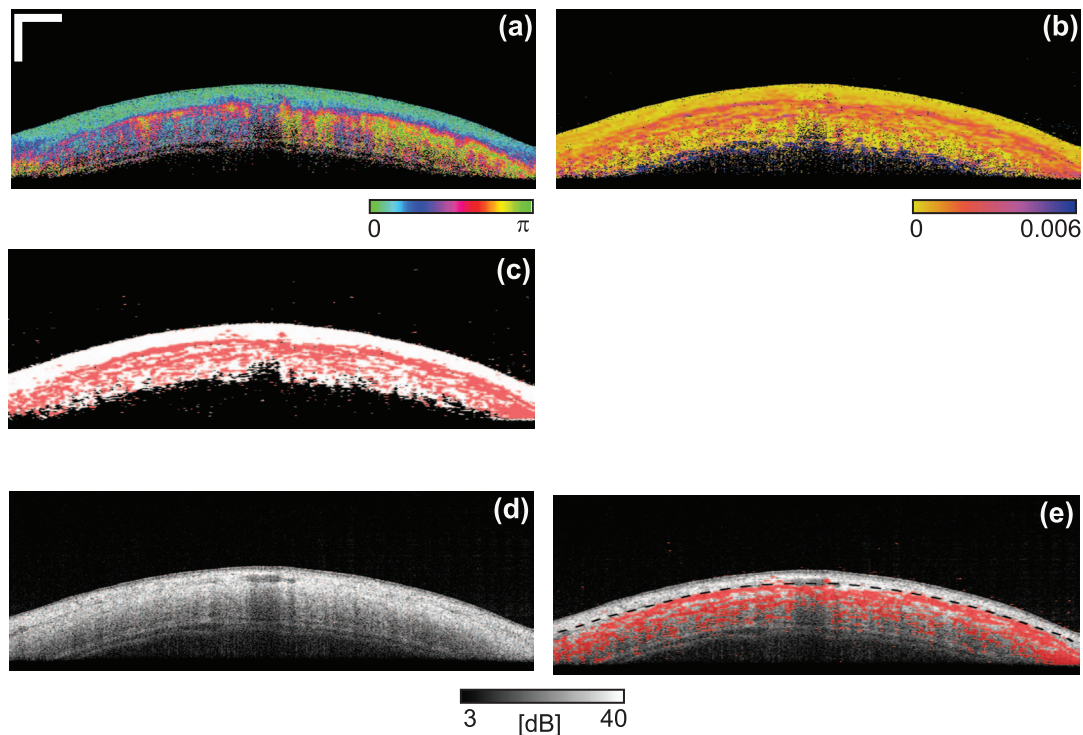


FIGURE 1. An example of normal anterior sclera. Cumulative phase retardation tomography (a), birefringence tomography (b), highly birefringent pixels (red) overlaid on valid pixel (white) (c), scattering OCT (d), and highly birefringent pixels (red) overlaid on scattering OCT (e). Scale bar: 1×1 mm.

fluid region in the bleb for FS calculations as this region has very low OCT signal, thus very low reliability.

To show the effectiveness of the birefringence threshold in separating the normal conjunctiva from the sclera, the birefringence threshold was applied to one of the normal reference cases (64-year-old female, IOP = 12 mm Hg). Figure 1 shows cumulative phase retardation (Fig. 1a), birefringence (Fig. 1b), highly birefringent pixels overlaid on valid pixels (white, Fig. 1c), scattering OCT (Fig. 1d) and highly birefringent pixels (red) overlaid on scattering OCT (Fig. 1e). The dotted line in Figure 1e is the manually delineated boundary between the conjunctiva and sclera. Note that the valid and highly birefringent pixels were defined not only at the conjunctival region but in the entire field of OCT in this particular demonstration. Figure 1e demonstrates the effective separation of conjunctiva and sclera based on birefringence.

Subjects and Protocol

The study included 20 subjects (12 males and eight females) who had undergone filtration surgery: 11 cases of primary open angle glaucoma (POAG), 6 of pseudoexfoliative glaucoma (PEG), 1 of neovascular glaucoma (NVG), 1 of primary angle closure glaucoma (ACG), and 1 of drug-induced secondary glaucoma (SG). Of these cases, 17 had undergone trabeculectomy and three had undergone Ex-PRESS tube shunt surgery. The details of the surgical protocols have been described previously.¹⁵

The mean age of the patients was 69.8 ± 13.4 years. The mean time period between filtration surgery and PS-OCT imaging was 3.42 ± 4.21 years (range, 1 day to 14.3 years).

According to IOP and involvement of ocular hypotensive agent, a case was classified as functional if IOP ≤ 18 mm Hg, or nonfunctional if IOP > 18 mm Hg. However, all cases in which ocular hypotensive agent was prescribed were classified as

nonfunctional irrespective of the IOP. Intraocular pressure was measured by Goldmann applanation tonometry on the day of PS-OCT imaging.

Polarization-sensitive OCT 3-D volumes of the filtering blebs were obtained for each subject. A volume covered a 12×12 mm transversal area and consisted of 512 (horizontal) $\times 128$ (vertical) A-lines. The volume was acquired with a horizontal fast raster scanning protocol. The imaging site of the bleb was chosen on the basis of the square scleral flap and block suture for fornix-based conjunctival flap by slit-lamp biomicroscopy. In those subjects who had no visible scleral flap, a volumetric scan of a clinical anterior segment OCT (CASIA; Tomey Corp.) taken before PS-OCT measurement also was used to choose the imaging site. Two volumes were taken for each subject. One volume was selected randomly for each subject, and used to compute FS. The other volumes were used to validate the reproducibility.

The bleb measurement was performed by experienced ophthalmologists at the University of Tsukuba Hospital (Tsukuba, Ibaraki, Japan). This study followed the tenets of the Declaration of Helsinki and informed consent was obtained before PS-OCT imaging. The study was approved by the Institutional Review Board of the University of Tsukuba.

The FS was computed for 10 cross-sections, including five equally-spaced horizontal and five vertical cross-sections, for each bleb. The average of these 10 FSs then was used as the FS of the bleb.

Statistical Analysis

The difference in the mean FS between the functional and nonfunctional bleb groups was evaluated by Welch's *t*-test. The correlation of FS with age, IOP, and the time interval from the surgery to PS-OCT imaging was examined by Pearson's correlation test. The capability of FS to discriminate nonfunc-

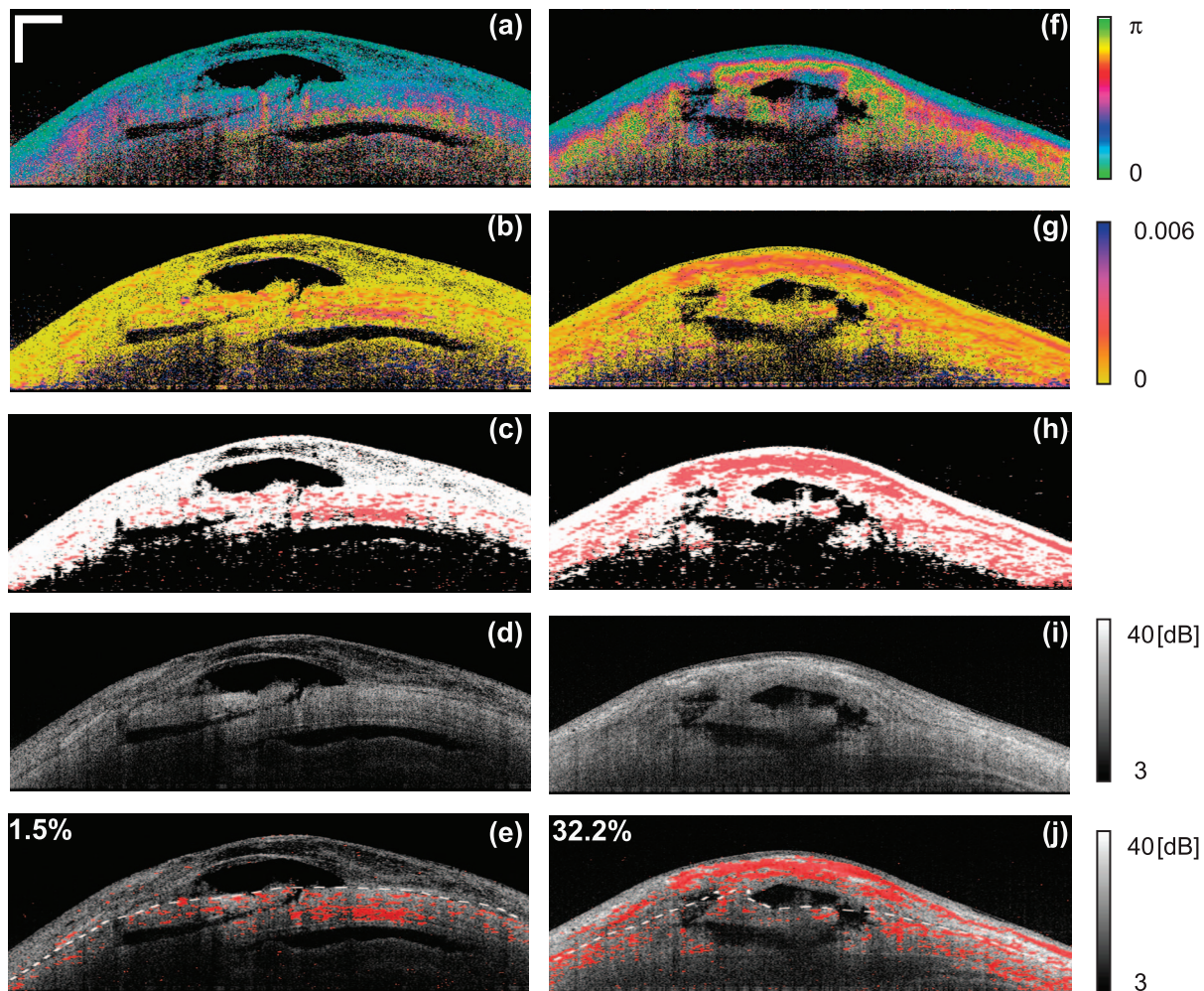


FIGURE 2. The example cases of functional bleb (*left column*) and nonfunctional bleb (*right column*). Each raw image represents cumulative phase retardation tomography (a) and (f), birefringence tomography (b) and (g), highly birefringent pixels (red) overlaid on valid pixels (white; c) and (h), scattering OCT (d) and (i), and highly birefringent pixel (red) overlaid on scattering OCT (e) and (j). The numbers in (e) and (j) are the fibrosis scores of these cases. Scale bar: 1×1 mm.

tional from the functional blebs was evaluated by the area under the receiver operating characteristics curves (AROC). The reproducibility of FS is assessed by the coefficient of variation and intraclass correlation (ICC). The statistical analysis was performed by R (version 3.2.1), except for the AROC analysis. The AROC analysis was performed using a custom program written in FreeMat computation environment.

RESULTS

The left column of Figure 2 shows an example of a functional bleb (72-year-old male, 2.2 months after Ex-PRESS shunt surgery, IOP = 12 mm Hg) as cumulative phase retardation (Fig. 2a), birefringence (Fig. 2b), highly birefringent pixels overlaid on valid pixels (white, Fig. 2c), scattering OCT (Fig. 2d), and highly birefringent pixels (red) overlaid on scattering OCT (Fig. 2e). The white dotted line is the manually delineated boundary between the conjunctiva and sclera. The scattering OCT showed characteristic features of functional blebs, such as an extended, diffuse, spongy, and hyporeflective region in thickened conjunctiva. A very low FS of 1.5% was obtained for this particular cross-section, with an average FS of 5.2% over 10 cross-sections.

The right column of Figure 2 shows an example of a nonfunctional bleb case (69-year-old male, 5.8 months after trabeculectomy, IOP = 27 mm Hg, ocular hypotensive agent prescribed). The images are in the same order as the left column. A spongy conjunctival region was not observed in the scattering OCT (Fig. 2i). In addition, a large high birefringence region in the conjunctiva surrounded the bleb (Fig. 2j). The FS was as high as 32.2% for this cross-section, with an average FS of 30.7% for 10 cross-sections.

Figure 3 shows the box-and-whisker plot of FS for the functional and nonfunctional groups where the whisker indicates the whole range, the box indicates the 25-to-75 percentile range, the horizontal line in the box is the median, and the dot in the box is the mean. The mean FS was $10.03\% \pm 5.72\%$ for the functional case group, which was significantly higher than the mean FS of $21.33\% \pm 10.88\%$ for the nonfunctional group ($P = 0.0075$). The FS showed high repeatability as ICC = 0.93 with the 95% confidence interval of (0.84, 0.97). The coefficient of variation was 14.9% in average.

A significant moderately positive correlation was found between FS and IOP in the nonfunctional group ($r = 0.66$, $P = 0.019$), but not in the functional group ($r = 0.129$, $P = 0.76$).

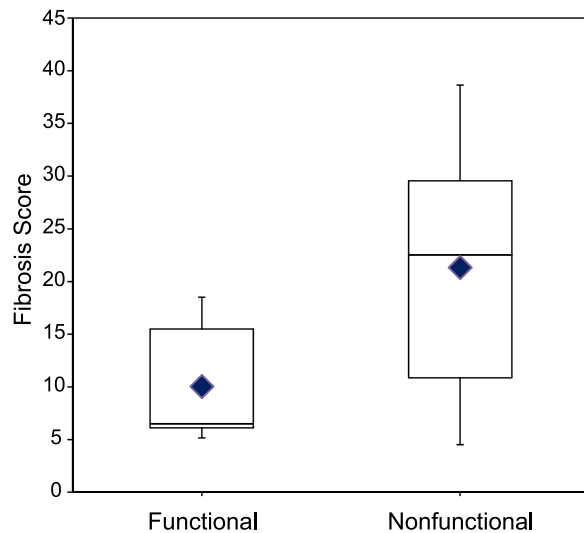


FIGURE 3. Fibrosis scores of the functional and nonfunctional group. The whiskers indicate the ranges of FS. The boxes indicate the 25-to-75 percentile regions, and the horizontal bars in the boxes are the medians. The dots in the boxes represent the mean FSs.

No significant correlation was found between FS and age ($r = -0.65$, $P = 0.081$ for the functional group, and $r = 0.68$, $P = 0.83$ for the nonfunctional group) and between FS and time-after-surgery ($r = 0.11$, $P = 0.80$ for the functional group, and $r = -0.40$, $P = 0.20$ for the nonfunctional group).

Figure 4 shows a receiver operating characteristic curve of FS for its capability to discriminate nonfunctional from the functional cases, where the sensitivity is defined as the correct classification rate of nonfunctional cases. The AROC was 0.82. The examples of sensitivity and specificity were computed at three points on the ROC as (sensitivity = 67%, specificity = 100%) at the point indicated by circle in Figure 4, which is the minimum distance point from the upper left corner of the plot (67%, 62.5%) at the square symbol and (92%, 62.5%) at the triangle symbol.

DISCUSSION

Although PS-OCT has been used previously as an imaging tool for bleb evaluation,¹³⁻¹⁵ this evaluation was based on cumulative phase retardation imaging. The cumulative phase retardation is not a direct measure of birefringence. Namely, tissue birefringence obtained through phase retardation analysis is not accurate if the tissue has a randomly-oriented fibrous structure, such as in the case of fibrosis in the bleb. It has been known empirically, and recently had been mathematically formulated.²⁵ Hence, the present method of local birefringence analysis was used to provide accurate birefringence even for such tissues.

The previous bleb classification schemes are based mainly on the morphologic features of the bleb.¹¹ The method of the present study is based on the direct imaging of tissue alteration in its birefringence. It visualizes the extent of fibrosis, and, hence, it more directly reflects the functionality of the bleb than the morphologic features visualized by scattering OCT. Since PS-OCT is noncontact and noninvasive, it enables frequent and periodic follow-up of the bleb. Moreover, PS-OCT imaging is possible even just after surgery without risk of infection, unlike UBM.

Although previous anterior segment OCT highlighted some causes of the obstruction of aqueous humor flow in the

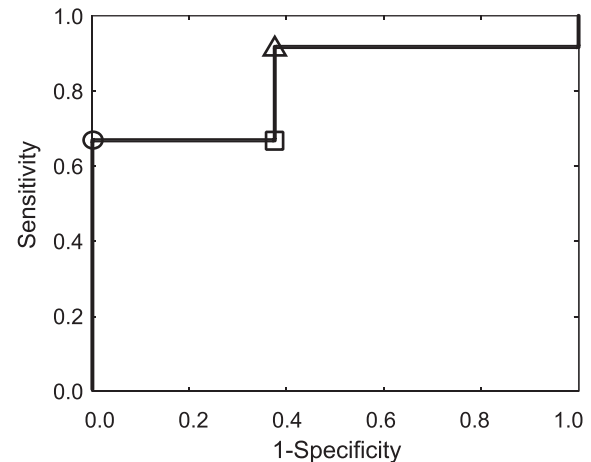


FIGURE 4. The receiver operating characteristic curve of the FS. The sensitivity is that to differentiate nonfunctional bleb from functional bleb.

bleb,^{9,26} there still is no clear strategy to assure successful needling revision or repeated filtration surgery. Recently, local birefringence imaging was used to monitor blebs before and after needling revision.¹⁸ Since the local birefringence imaging selectively visualizes the fibrosis, it is useful to optimize the needling surgery. The FS provides an objective measure of the fibrosis in addition to the qualitative birefringence imaging, and would further optimize the needling surgery.

There are several bleb revision surgery methods.²⁷ The FS would help in selection of revision methods. In addition, the FS can be used to monitor the progression of fibrosis with novel anti-fibrotic agents.²⁸

The present method has certain limitations for evaluation of blebs with strong inflammation and congestion. In our previous rabbit study,¹⁴ we have seen no increase in phase retardation 0 days after surgery compared to 1 and 2 weeks after the surgery. This evidently suggests that the inflammation does not affect phase retardation and birefringence. Although inflammation and congestion may not directly affect birefringence, the change in the volume of conjunctiva during inflammation and congestion might affect the FS. This is a limitation of our current method.

The current FS computation involves manual delineation of the conjunctiva and sclera, and it increases the analysis time and effort. It also restricts the analysis into quasi-3-D analysis; only 10 cross-sections are analyzed for each volume. Full 3-D analysis will make the FS more sensitive to localized fibrosis. Automatic segmentation is required to further improve the sensitivity and use of the FS.

Although the present study showed a sensitivity of 67% and specificity of 100%, it is based on only a small-scale pilot study. A larger case study is essential to further qualify the FS. In addition, the subjects included in this study were imaged at different time periods after filtration surgery, and, hence the state of the bleb would have large variation. This is another shortcoming of the current small-scale study. This limitation could be analyzed further by more specific studies. One could be a large-scale study only with old blebs, which could provide an optimized use of FS for better reintervention. The other study would be a longitudinal study to see the long-time evolution of FS from just after the surgery to several years. This would provide an interpretation scheme of FS to predict the functionality of bleb.

In the present study, localized birefringence imaging was used to assess quantitatively the bleb created by filtration

surgery. A birefringence-based metric, the FS, was defined for this quantitative assessment. The present pilot study showed good capability of the FS to differentiate between functional and nonfunctional blebs. A further large-scale study would establish the practical clinical use of birefringence imaging and FS for glaucoma surgery.

Acknowledgments

Supported in part by Japan Society for the Promotion of Science through the contract of KAKENHI 2503053 and Tomey Corporation.

Disclosure: **D. Kasaragod**, Tomey Corp. (F), Topcon Corp. (F), Nidek (F); **S. Fukuda**, None; **Y. Ueno**, None; **S. Hoshi**, None; **T. Oshika**, Tomey Corp. (F); **Y. Yasuno**, Tomey Corp. (F), Topcon Corp. (F), Nidek (F), P

References

1. The Advanced Glaucoma Intervention Study (AGIS): 7. The relationship between control of IOP and visual field deterioration. *Am J Ophthalmol*. 2000;1304:429-440.
2. Skuta GL, Parrish RK. Wound healing in glaucoma filtering surgery. *Surv Ophthalmol*. 1987;32:149-170.
3. Grehn F, Picht G, Lüssen UW, Lütjen-Drecoll E. Wound healing and scarring of the developing filtering bleb — a major challenge in glaucoma surgery. In: Gramer PD, Grehn PD, eds. *Pathogenesis and Risk Factors of Glaucoma*. Berlin: Springer; 1999:50-56.
4. Khaw PT, Chang L, Wong TT, Mead A, Daniels JT, Cordeiro MF. Modulation of wound healing after glaucoma surgery. *Curr Opin Ophthalmol*. 2001;12:143-148.
5. Yu-Wai-Man C, Khaw PT. Developing novel anti-fibrotic therapeutics to modulate post-surgical wound healing in glaucoma: big potential for small molecules. *Expert Rev Ophthalmol*. 2015;10:65-76.
6. Wells AP, Cordeiro MF, Bunce C, Khaw PT. Cystic bleb formation and related complications in limbus- versus fornix-based conjunctival flaps in pediatric and young adult trabeculectomy with mitomycin C. *Ophthalmology*. 2003;110:2192-2197.
7. Wells AP, Crowston JG, Marks J, et al. A pilot study of a system for grading of drainage blebs after glaucoma surgery. *J Glaucoma*. 2004;13:454-460.
8. Morita K, Gao Y, Saito Y, et al. In vivo confocal microscopy and ultrasound biomicroscopy study of filtering blebs after trabeculectomy: limbus-based versus fornix-based conjunctival flaps. *J Glaucoma*. 2012;21:383-391.
9. Singh M, Chew PTK, Friedman DS, et al. Imaging of trabeculectomy blebs using anterior segment optical coherence tomography. *Ophthalmology*. 2007;114:47-53.
10. Kawana K, Kiuchi T, Yasuno Y, Oshika T. Evaluation of trabeculectomy blebs using 3-dimensional cornea and anterior segment optical coherence tomography. *Ophthalmology*. 2009;116:848-855.
11. Wells AP, Ashraff NN, Hall RC, Purdie G. Comparison of two clinical bleb grading systems. *Ophthalmology*. 2006;113:77-83.
12. Cantor LB, Mantravadi A, WuDunn D, Swamynathan K, Cortes A. Morphologic classification of filtering blebs after glaucoma filtration surgery: the Indiana Bleb Appearance Grading Scale. *J Glaucoma*. 2003;12:266-271.
13. Yasuno Y, Yamanari M, Kawana K, Oshika T, Miura M. Investigation of post-glaucoma-surgery structures by three-dimensional and polarization sensitive anterior eye segment optical coherence tomography. *Opt Express*. 2009;17(5):3980-3995.
14. Lim Y, Yamanari M, Fukuda S, et al. Birefringence measurement of cornea and anterior segment by office-based polarization-sensitive optical coherence tomography. *Biomed Opt Express*. 2011;2:2392-2402.
15. Fukuda S, Beheregaray S, Kasaragod D, et al. Noninvasive evaluation of phase retardation in blebs after glaucoma surgery using anterior segment polarization-sensitive optical coherence tomography. *Invest Ophthalmol Vis Sci*. 2014;55:5200-5206.
16. Makita S, Yamanari M, Yasuno Y. Generalized Jones matrix optical coherence tomography: performance and local birefringence imaging. *Opt Express*. 2010;18:854-876.
17. Kasaragod D, Makita S, Fukuda S, Beheregaray S, Oshika T, Yasuno Y. Bayesian maximum likelihood estimator of phase retardation for quantitative polarization-sensitive optical coherence tomography. *Opt Express*. 2014;22:16472-16492.
18. Yamanari M, Tsuda S, Kokubun T, et al. Fiber-based polarization-sensitive OCT for birefringence imaging of the anterior eye segment. *Biomed Opt Express*. 2015;6:369.
19. Ju MJ, Hong YJ, Makita S, et al. Advanced multi-contrast Jones matrix optical coherence tomography for Doppler and polarization sensitive imaging. *Opt Express*. 2013;21:19412-19436.
20. Baumann B, Götzinger E, Pircher M, Hitzenberger CK. Single camera based spectral domain polarization sensitive optical coherence tomography. *Opt Express*. 2007;15:1054.
21. Miyazawa A, Yamanari M, Makita S, et al. Tissue discrimination in anterior eye using three optical parameters obtained by polarization sensitive optical coherence tomography. *Opt Express*. 2009;17:17426-17440.
22. Shields JA, Eagle RC, Shields CL, Green M, Singh AD. Systemic amyloidosis presenting as a mass of the conjunctival semilunar fold. *Am J Ophthalmol*. 2000;130:523-525.
23. Seet L-F, Lee WS, Su R, Finger SN, Crowston JG, Wong TT. Validation of the glaucoma filtration surgical mouse model for antifibrotic drug evaluation. *Mol Med*. 2011;17:557-567.
24. Otsu N. A threshold selection method from gray-level histograms. *IEEE Trans Syst Man Cybern*. 1979;9:62-66.
25. Sugiyama S, Hong YJ, Kasaragod D, et al. Birefringence imaging of posterior eye by multi-functional Jones matrix optical coherence tomography. *Biomed Opt Express*. 2015;6:4951.
26. Nakano N, Hangai M, Nakanishi H, et al. Early trabeculectomy bleb walls on anterior-segment optical coherence tomography. *Graefes Arch Clin Exp Ophthalmol*. 2010;48:1173-1182.
27. La Borwit SE, Quigley HA, Jampel HD. Bleb reduction and bleb repair after trabeculectomy. *Ophthalmology*. 2000;107:712-718.
28. Butler MR, Prospero Ponce CM, Weinstock YE, Orengo-Nania S, Chevez-Barrios P, Frankfort BJ. Topical silver nanoparticles result in improved bleb function by increasing filtration and reducing fibrosis in a rabbit model of filtration surgery. *Invest Ophthalmol Vis Sci*. 2013;54:4982-4990.